Neuron, Volume *107*

Supplemental Information

Soma-Targeted Imaging of Neural Circuits by Ribosome Tethering

Yiming Chen, Heeun Jang, Perry W.E. Spratt, Seher Kosar, David E. Taylor, Rachel A. Essner, Ling Bai, David E. Leib, Tzu-Wei Kuo, Yen-Chu Lin, Mili Patel, Aygul Subkhangulova, Saul Kato, Evan H. Feinberg, Kevin J. Bender, Zachary A. Knight, and Jennifer L. Garrison

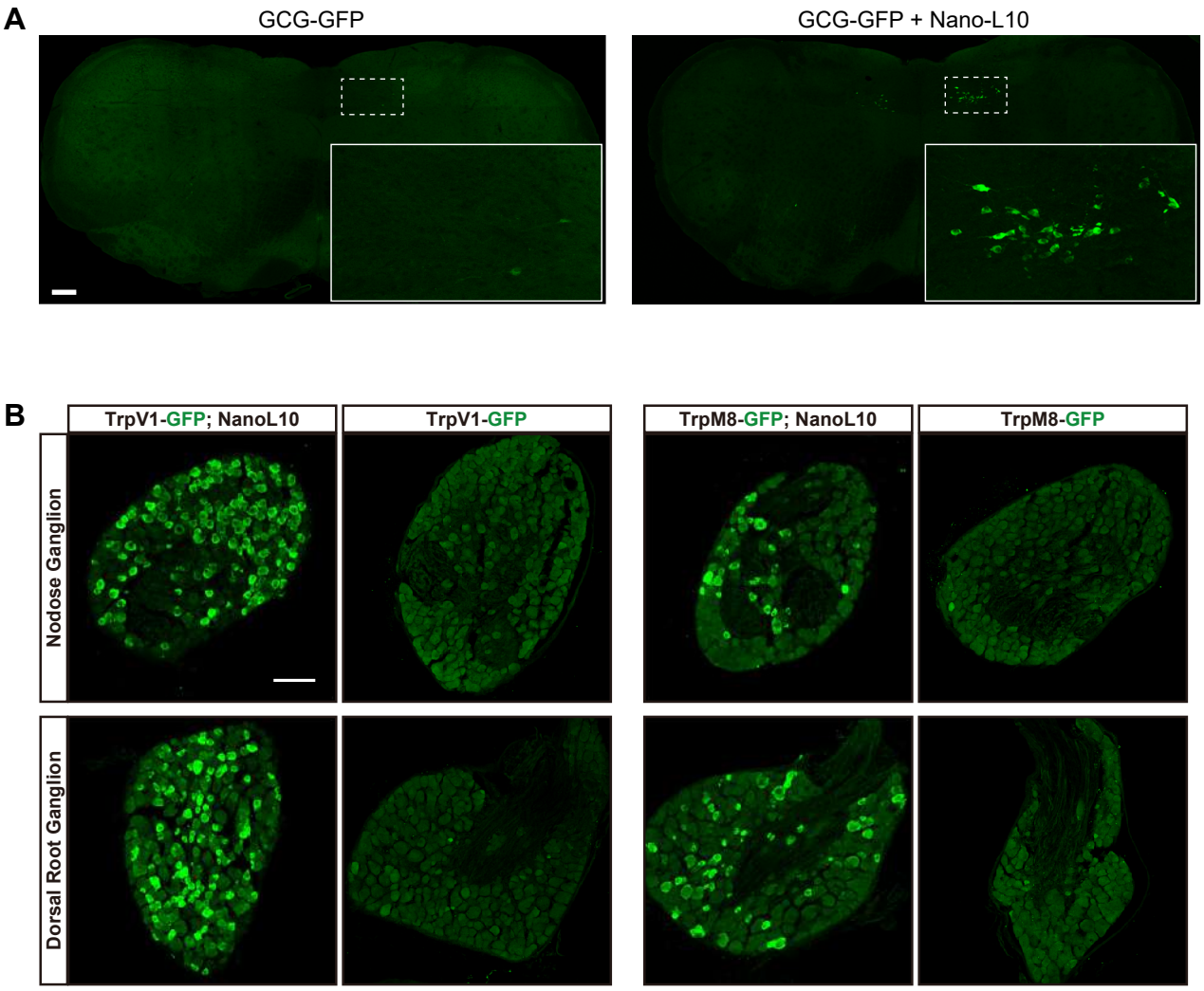

Figure S1: Nano-L10 amplifies the fluorescence of GFP reporter mice. Related to Figure 1.

(A) Direct fluorescence from a coronal slice of the brain stem of GCG-GFP mice (left) and GCG-GFP+Nano-L10 mice (right). GCG neurons are in the caudal solitary tract are shown in the inset. This is the same region shown in Figure 1E, reproduced here with the entire coronal slice for context. Scale bar indicates 200 μm.
(B) Fluorescence from nodose and dorsal root ganglia of TRPV1-GFP-DTR and TRPM8-GFP-DTR mice with and without co-expression of Nano-L10. These images are after GFP immunostaining. The same sections are shown in Figure 1F, G as native fluorescence. Scale bar indicates 100 μm.

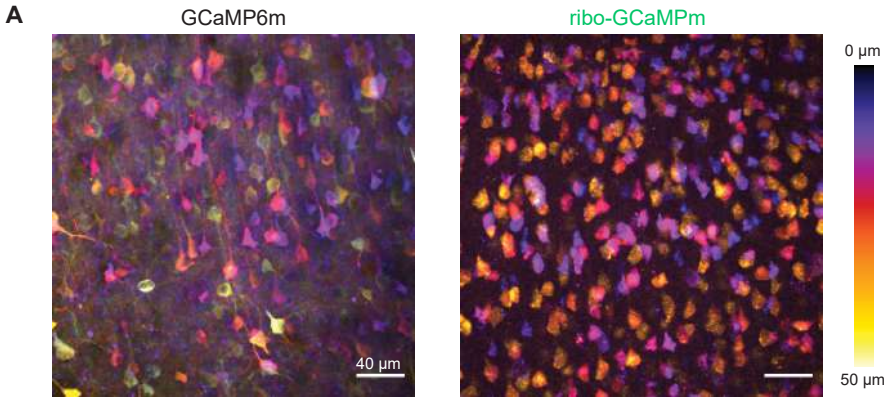

Figure S2. Ribo-tagging confines the fluorescence of GCaMP to soma of neurons. Related to Figure 4.
(A) 2-photon z-stack of non-calcium bound GCaMP6m fluorescence in medial prefrontal cortex, with 810nm imaging wavelength, which readily excites GCaMP6m in the non-calcium bound state. Pseudocolor indicates the depth of each pixel in the z-plane.

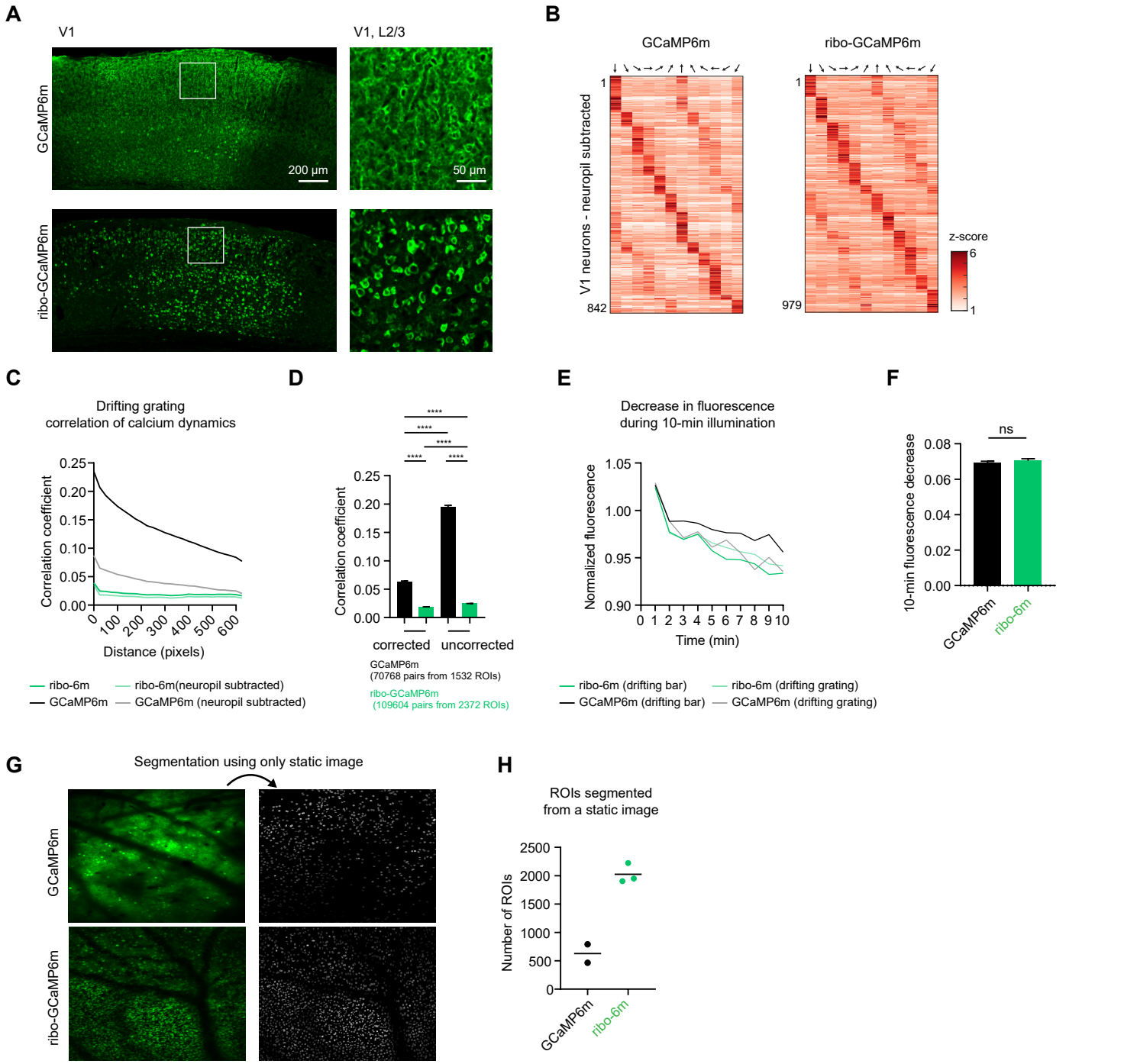

Figure S3. Ribo-GCaMP reduces contamination from neuropil during 2-photon imaging. Related to Figure 5.
(A) Immunohistology of GCaMP6m (top) and ribo-GCaMP6m (bottom) expression in V1.
(B) Peak response of angle-selective V1 neurons to drifting gratings with different angles.
(C-D) Correlation coefficient analysis of neural signal reported by either GCaMP6m or ribo-GCaMP6m. Neuropil signal was either subtracted or not. During recording, mice were exposed to drifting gratings.
(C) Correlation coefficient of temporal calcium dynamics between pairs of neurons plotted against centroid distance. R^2 = 0.92, 0.33, 0.85 and 0.22, p: <0.0001, 0.0014, <0.0001 and 0.0121 for regular uncorrected, ribo uncorrected, regular, and ribo respectively, linear regression of averaged values.
(D) Correlation coefficent of temporal calcium dynamics between pairs of neurons that are within 100 pixels. Regular corrected: 0.06 ± 0.02; ribo corrected: 0.02 ± 0.000; regular uncorrected: 0.20 ± 0.003; ribo uncorrected: 0.02 ± 0.000; values are Mean ± SEM. ****: p < 0.0001, 1-way ANOVA, Holm-Sidak post-hoc test. Total numbers of cells were used to estimate degrees of freedom when calculating S.E.M.
(E-F) Timecourse of fluorescence throughout a 10-minute recording (E) and quantification of the total fluorescence decrease after recording (drifting-bar and drifting-grating experiments are pooled) (F) ns: p > 0.05, unpaired t-test. In E-F, the fluorescence intensity of each ROI is normalized to the median of intensity during the first minute of recording. Traces of all ROIs in each experiment recorded for each ribo-GCaMP6m or GCaMP6m are averaged to generate each plot in E. Percentage decrease (i.e. extent of bleaching) of all ROIs from all experiments are pooled for ribo-GCaMP6m (n = 4,732) or GCaMP6m (n = 3,032) and compared in F.
(G) Image showing the average z-projection of two-photon recording of V1 neurons expressing GCaMP6m (top) and ribo-GCaMP6m (bottom). The same image underwent NeuroSeg for automated segmentation that does not rely on time-series data.
(H) Number of ROIs identified with NeuroSeg in data recorded with GCaMP6m (n = 2 videos) and ribo-GCaMP6m (n = 3 videos).

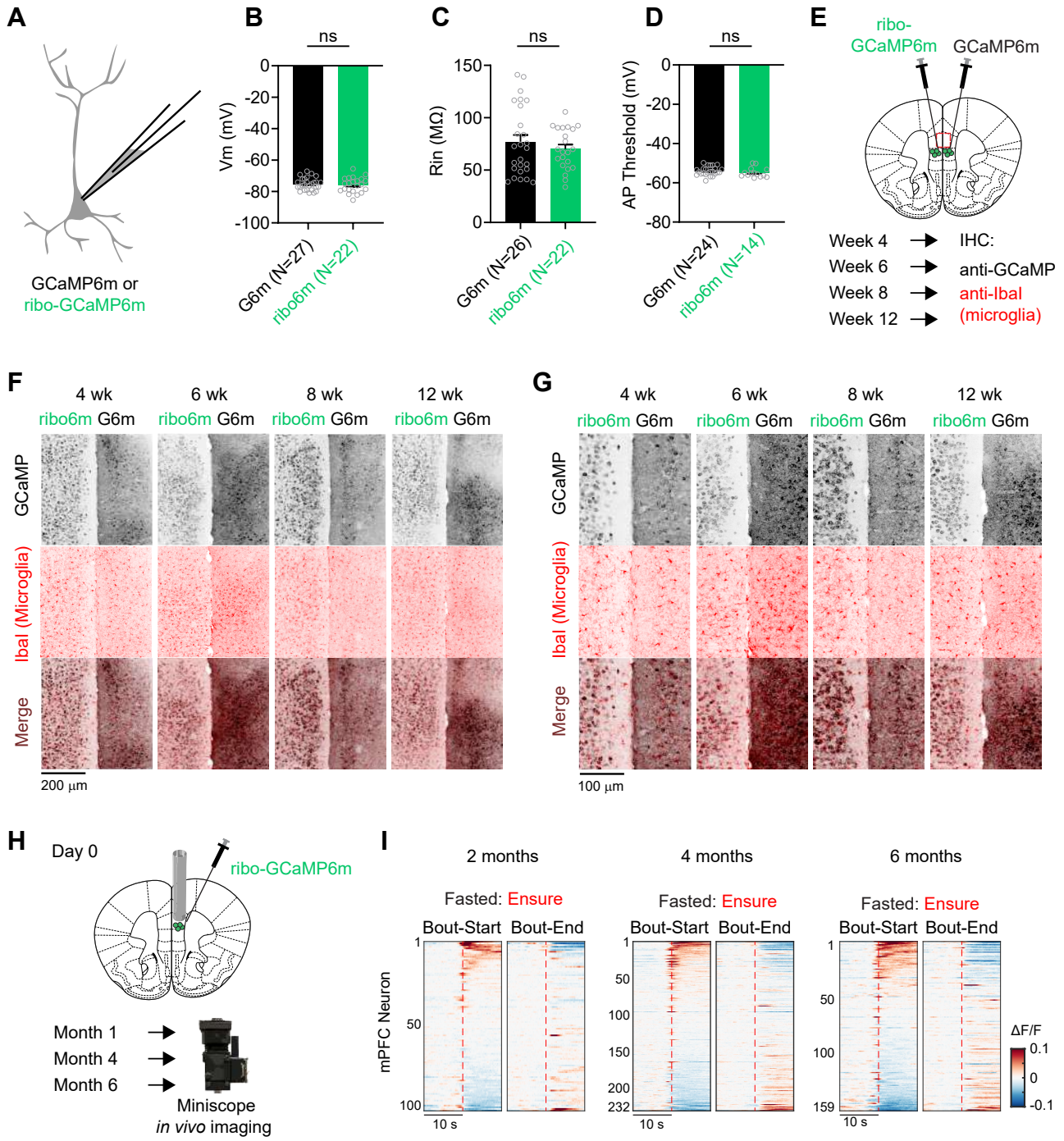

Figure S4. Ribo-GCaMP6m does not cause detectable toxicity. Related to Figure 6.
(A) PFC cells expressing ribo-GCaMP6m or GCaMP6m were characterized by patch clamp electrophysiology.
(B-D) Resting membrane potential (B), input resistance (C) and spiking thresholds (D) of cells expressing ribo-GCaMP6m (green) and GCaMP6m (black). ns: $p > 0.05$, unpaired t-test.
(E) Accessing neural toxicity of ribo-GCaMP6m and GCaMP6m through immunohistochemistry.
(F and G) Expression pattern and microglia distribution after allowing ribo-GCaMP6m or GCaMP6m to be expressed for 4, 6, 8 and 12 months, shown with different magnification. Scale bar sizes are indicated for each panel.
(H) Accessing neural toxicity of ribo-GCaMP6m through chronic microendoscope imaging
(I) Response of mPFC neurons to food consumption after allowing ribo-GCaMP6m to be expressed for 2, 4 and 6 months. Each line represents averaged PSTH of neural activity aligned to start or end of feeding bouts of neuron.

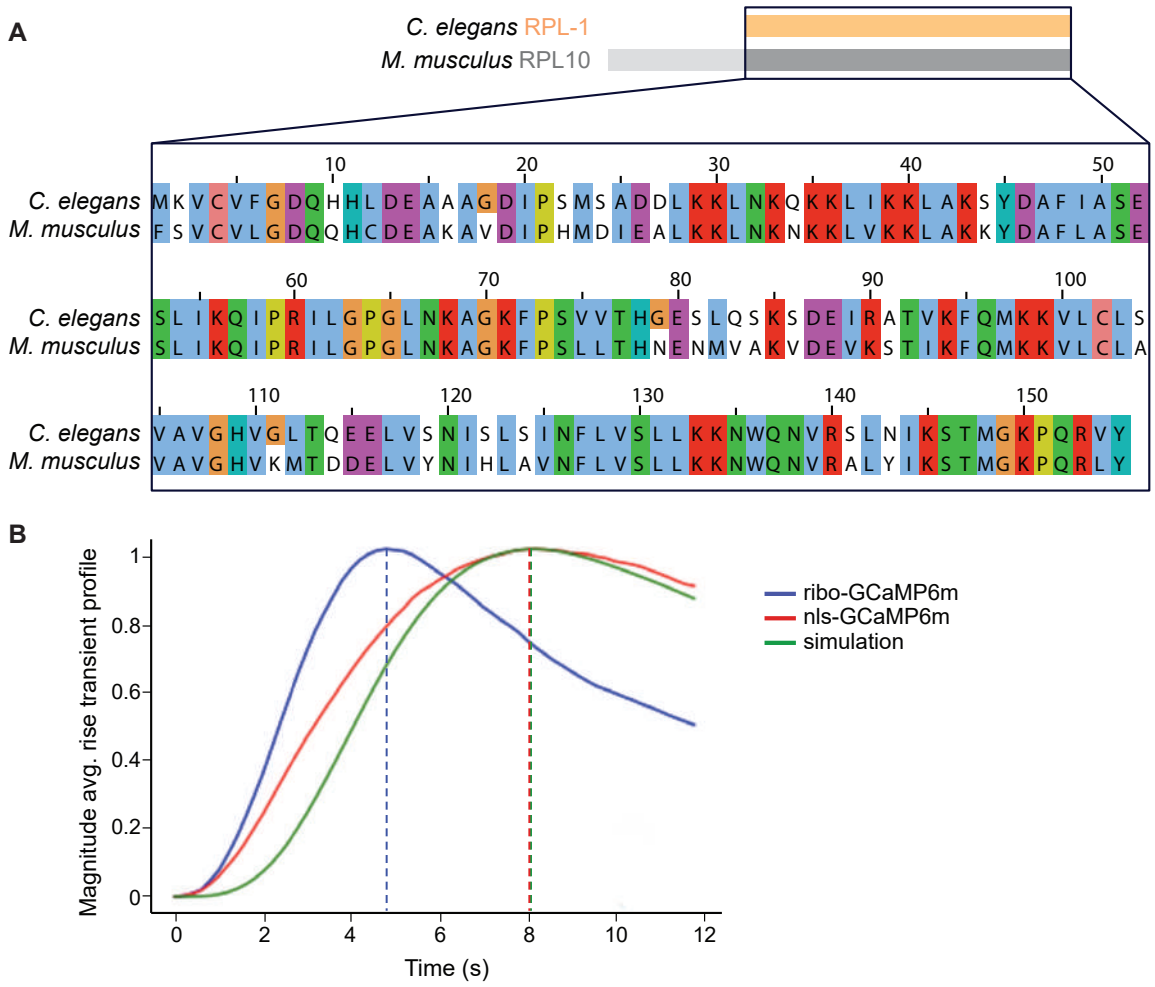

Supplementary Figure S5. **A soma-targeted GCaMP enables imaging in C. elegans. Related to Figure 7.**
(A) Sequence alignment of ribosomal proteins used for ribo-GCaMP6m expression in worms. GCaMP6m was tethered to *C. elegans* ribosomal protein 1a (RPL-1), which shares 75% amino acid identity and 88% similarity with mouse protein L10. *C. elegans* RPL-1 (Q95Y46_CAEEL) amino acids 1-155 and *M. Musculus* RPL10 (C5XJF6_MOUSE) amino acids 63-217 were aligned using Jalview2 (Waterhouse, et al., 2009) and shaded according to the Clustal X color scheme.
(B) Modeling the delayed rise time kinetics observed for nls-GCaMP6m in *C. elegans*. An effective transformation between nls-GCaMP6m (red line) and ribo-GCaMP6m (blue line) traces was modeled as a single-exponential linear filter (green line), followed by estimation of the time constant of the best-fit filter across all the distributions of rise transients giving a filter time constant of 3.2 s.

SUPPLEMENTAL VIDEOS

Movie S1. 2-photon imaging of primary visual cortex (V1) with GCaMP6m. Related to Figure 5.
A representative field of view from V1 recorded using 2-photon microscopy. Mice were exposed to drifting bars with different orientation as visual stimuli. Neurons express GCaMP6m. This video shows the same field of view as in Figure 5A.

Movie S2. 2-photon imaging of primary visual cortex (V1) with GCaMP6m. Related to Figure 5.
A representative field of view from V1 recorded using 2-photon microscopy. Mice were exposed to drifting bars with different orientation as visual stimuli. Neurons express GCaMP6m.

Movie S3. 2-photon imaging of primary visual cortex (V1) with ribo-GCaMP6m. Related to Figure 5.
A representative field of view from V1 recorded using 2-photon microscopy. Mice were exposed to drifting bars with different orientation as visual stimuli. Neurons express ribo-GCaMP6m. This video shows the same field of view as in Figure 5A.

Movie S4. 2-photon imaging of primary visual cortex (V1) with ribo-GCaMP6m. Related to Figure 5.
A representative field of view from V1 recorded using 2-photon microscopy. Mice were exposed to drifting bars with different orientation as visual stimuli. Neurons express ribo-GCaMP6m.

Movie S5. Whole-brain widefield calcium imaging of *C. elegans* basal neuronal activity. Related to Figure 8.
A representative maximum intensity projection movie of worms recorded under constant conditions. Neurons express nls-GCaMP6m. 1.5 min sped up 5X, scale bar = 10 μm.

Movie S6. Whole-brain widefield calcium imaging of *C. elegans* basal neuronal activity. Related to Figure 8.
A representative maximum intensity projection movie of worms recorded under constant conditions. Neurons express ribo-GCaMP6m. 1.5 min sped up 5X, scale bar = 10 μm.

Please cite this article in press as: Chen et al., Soma-Targeted Imaging of Neural Circuits by Ribosome Tethering, Neuron (2020), https://doi.org/10.1016/j.neuron.2020.05.005

CellPress

STAR★METHODS

KEY RESOURCES TABLE

REAGENT or RESOURCE	SOURCE	IDENTIFIER
Antibodies		
Chicken anti-GFP	Abcam	Abcam Cat# ab13970, RRID:AB_300798
Rabbit anti-Iba1	Wako	Wako Cat# 019-19741, RRID:AB_839504
Goat anti-chicken Alexa 488	Invitrogen	Thermo Fisher Scientific Cat# A-11039, RRID:AB_2534096
Goat anti-rabbit Alexa 568	Invitrogen	Thermo Fisher Scientific Cat# A-11036, RRID:AB_10563566
Bacterial and Virus Strains		
AAV5- EF1a-DIO-hChR2(H134R)-mCherry-WPRE-HGHpA	Gift from Karl Deisseroth; unpublished	Karl Deisseroth Addgene plasmid #20297
Plasmid: pAAV-hSyn-GCaMP6m-RPL10a-WPRE-HGH	This paper; AAV8 produced by Stanford Vector Core	N/A
Plasmid: pAAV-hSyn-GCaMP6f-RPL10a-WPRE-HGH	This aper; AAV8 produced by Stanford Vector Core	N/A
Plasmid: pAAV-hSyn-GCaMP6s-RPL10a-WPRE-HGH	This paper; AAV8 produced by Stanford Vector Core	N/A
Plasmid: pAAV-hSyn-GCaMP6m-WPRE-HGH (control vector)	This paper; AAV8 produced by Stanford Vector Core	N/A
Plasmid: pAAV-hSyn-DIO-GCaMP6m-RPL10a-WPRE-HGH	This paper; AAV8 produced by Stanford Vector Core	N/A
Plasmid: pAAV-hSyn-DIO-GCaMP6f-RPL10a-WPRE-HGH	This paper; AAV5 produced by Stanford Vector Core	N/A
Plasmid: pAAV-hSyn-DIO-GCaMP6s-RPL10a-WPRE-HGH	This paper	N/A
Chemicals, Peptides, and Recombinant Proteins		
CNQX	Tocris	Cat# 0190
(R)-CPP	Tocris	Cat# 00247
Gabazine	Tocris	Cat# 01262
(S)-MCPG	Tocris	Cat# 00337
Tetramisole Hydrochloride	Sigma-Aldrich	CAS# 5086-74-8
DAPI fluoromount-G	Southern Biotech	Cat# 0100-20
Experimental Models: Organisms/Strains		
M. musculus: C57BL/6J (WT)	JAX	JAX: 000664, RRID: IMSR_JAX:000664
M. musculus: Tg(Sim1-cre)1Lowl/J (SIM1-Cre)	JAX	JAX: 006395, RRID: IMSR_JAX:006395
M. musculus: Tg(Agtr1a-EGFP)NZ44Gsat (Agtr1a-EGFP)	GENSAT	MGI:4846843
GCG-GFP	Gift from Hayashi Yoshitaka; Hayashi et al., 2009	N/A
GAD67-GFP	Gift from Allan Basbaum, Tamamaki et al., 2003	N/A
TrkB-tauGFP	Gift from David Ginty; Li et al., 2011	N/A
TRPV1-GFP-DTR	Gift from Mark Hoon; Pogorzala et al., 2013	N/A
TRPM8-GFP-DTR	Gift from Mark Hoon; Pogorzala et al., 2013	N/A
Nano-L10	Ekstrand et al., 2014	N/A

(*Continued on next page*)

Please cite this article in press as: Chen et al., Soma-Targeted Imaging of Neural Circuits by Ribosome Tethering, Neuron (2020), https://doi.org/10.1016/j.neuron.2020.05.005

Continued

REAGENT or RESOURCE	SOURCE	IDENTIFIER
M. musculus: B6;129S4-Ntrk1tm1(cre)Lfr/Mmucd (Ntrk1-Cre)	MMRRC	RRID: MMRRC_015500-UCD
C. elegans: Strain N2	Caenorhabditis Genetics Center	WB Strain: 00000001
C. elegans: Strain KG1180: *lite-1(ce314) X.*	Caenorhabditis Genetics Center	WB Strain: 00023485
C. elegans: Strain JAZ279: *jIgEx289[Psra6::GCaMP6m::rpl-1a;Punc-122::dsRed2]*	This study	N/A
C. elegans: Strain JAZ312: *jIgEx301[Psra6::GCaMP6m;Punc-122::GFP]*	This study	N/A
C. elegans: Strain JAZ275: *jIgEx285[Pntc-1::GCaMP6m::rpl-1a;Punc-122::dsRed2]*	This study	N/A
C. elegans: Strain JAZ276: *lite-1(ce314) X; jIgEx286[Ptag-168::GCaMP6m::rpl1a;Punc-122::dsRed2];otIs355 [Prab3::2xNLS::tagRFP]*	This study	N/A
C. elegans: Strain JAZ313: *lite-1(ce314) X; jIgEx302[Prab-3::GCaMP6m::rpl1a;Pelt-2::2xNLS::GFP];otIs355 [Prab3::2xNLS::tagRFP]*	This study	N/A
Software and Algorithms		
FIJI	Schindelin et al., 2012	https://imagej.net/Fiji/Downloads
Psychtoolbox3	Kleiner et al., 2007	https://github.com/Psychtoolbox-3/Psychtoolbox-3
NormCorre	Pnevmatikakis and Giovannucci, 2017	https://github.com/flatironinstitute/NoRMCorre
Suite2P	Pachitariu et al., 2017	https://github.com/cortex-lab/Suite2P
Capacitive Sensing Library	Arduino Playground	https://playground.arduino.cc/Main/CapacitiveSensor/
CNMF_E	Zhou et al., 2018	https://github.com/zhoupc/CNMF_E
PCA/ICA	Mukamel et al., 2009	https://github.com/mukamel-lab/CellSort
NeuroSeg	Guan et al., 2018	https://github.com/baidatong/NeuroSeg
PRISM 7	GraphPad	https://www.graphpad.com RRID:SCR_005375
Mosaic	Inscopix	https://support.inscopix.com/mosaic-workflow RRID:SCR_017408
MATLAB R2019a	MathWorks	https://www.mathworks.com
MATLAB (Custom Code)	Available upon reasonable request	N/A
Python (Custom Code)	This study	https://github.com/focolab/ribo-gcamp/
Other		
Ø500 μm gradient index (GRIN) lens (6.1 mm length)	Inscopix	N/A

RESOURCE AVAILABILITY

Lead Contact

Further information about resources, reagents, and code should be directed to and will be fulfilled by the Lead Contact, Zachary Knight (zachary.knight@ucsf.edu).

Materials Availability

Plasmids generated in this study will be deposited at Addgene. Transgenic worm strains generated in this study will be deposited at the Caenorhabditis Genetics Center (CGC) and will be available within six months of publication.

Data and Code Availability

The datasets and code generated during this study are available from the Lead Contact without restriction.

Please cite this article in press as: Chen et al., Soma-Targeted Imaging of Neural Circuits by Ribosome Tethering, Neuron (2020), https://doi.org/10.1016/j.neuron.2020.05.005

EXPERIMENTAL MODEL AND SUBJECT DETAILS

Mice

We obtained SIM1-Cre transgenic mice (Tg(Sim1-cre)1Lowl/J, #006395) and wild-type mice (C57BL/6J, #000664) from Jackson Laboratory. We obtained Agtr1a-GFP transgenic mice (Tg(Agtr1a-EGFP)NZ44Gsat, MGI:4846843) from the GENSAT project. GCG-GFP, GAD67-GFP, TrkB-tauGFP, TRPV1-GFP-DTR, TRPM8-GFP-DTR, and Nano-L10 mice have been described previously (Ekstrand et al., 2014; Hayashi et al., 2009; Li et al., 2011; Pogorzala et al., 2013; Tamamaki et al., 2003). We obtained Ntrk1-Cre knockin mice (B6;129S4-Ntrk1tm1(cre)Lfr/Mmucd, RRID: MMRRC_015500-UCD) from MMRRC. Adult mice (> 6 weeks old) of both sexes were used for experiments. All animals were maintained on a 12-h light/dark cycle and given *ad libitum* access to chow (PicoLab Rodent Diet 5053) and water. All procedures were conducted during the light cycle unless otherwise noted. All experimental protocols were approved by the University of California, San Francisco IACUC following the National Institutes of Health guidelines for the Care and Use of Laboratory Animals.

Worms

All *C. elegans* strains were cultivated using standard protocols in a 20°C incubator on nematode growth media (NGM) plates seeded with *Escherichia coli* OP50 bacteria as a food source. Young adult (Day 1 or 2) hermaphrodites were used for all experiments. Transgenic lines were constructed by injecting plasmids using standard techniques.

METHOD DETAILS

Protein engineering

To tether GCaMP6 and the GFP nanobody to ribosomes, GCaMP6m (Chen et al., 2013) or the GFP nanobody (Ekstrand et al., 2014; Rothbauer et al., 2006) was linked to ribosomal subunit protein RPL10 through a short linker of amino acid sequence SGRTQISSSS-FEF (Heiman et al., 2008). The resultant construct is GCaMP6-RPL10 and is referred to as ribo-GCaMP for simplicity in the paper. All constructs were designed using a combination of restriction cloning, Gibson Assembly and gBlock gene fragments (Integrated DNA Technologies). For *C. elegans* constructs, the sequence of *rpl-1* was fused to the C-terminus of GCaMP6m using an overlap PCR strategy. All regions that underwent PCR amplification were checked through sanger sequencing (GeneWitz; Elim Biopharm) following RCA-based amplification (GE Templiphi). Constructs were made into custom AAV through Stanford Vector Core:

AAV8-hSyn-GCaMP6m/f/s (Restriction Cloning: AscI & NheI)
AAV5/8-hSyn-riboGCaMP6m/f/s (Gibson Assembly + gBlock)
AAV5/8-hSyn-DIO-riboGCaMP6m/f/s (Restriction Cloning: AscI & NheI)
Linker-RL10 amino acid sequence:
SGRTQISSSSFEFSSKVSRDTLYEAVREVLHGNQRKRRKFLETVELQISLKNYDPQKDKRFSGTVRLKSTPRPKFSVCVLGDQQHCD
EAKAVDIPHMDIEALKKLNKNKKLVKKLAKKYDAFLASESLIKQIPRILGPGLNKAGKFPSLLTHNENMVAKVDEVKSTIKFQMKKVLC
LAVAVGHVKMTDDELVYNIHLAVNFLVSLLKKNWQNVRALYIKSTMGKPQRLY

General surgical procedures

All surgical procedures were performed in accordance with institutional guidelines for anesthesia and analgesia. In brief, mice were anesthetized with isoflurane and placed in a stereotaxic device with eyes covered with ophthalmic ointment. Buprenorphine SR (1.5 mg/kg), meloxicam (5 mg/kg), and dexamethasone (0.6 mg/kg) were administered systemically to prevent pain and brain edema. Bupavicaine was applied at the surgical site. Specific surgical procedures are described in the sections that follow.

Immunohistochemistry

General procedure: Mice were transcardially perfused with PBS followed by 10% formalin, brains were dissected, post-fixed in 10% formalin overnight at 4°C, and then washed 3x20 minutes with PBS at RT. Tissue was then cryoprotected with 30% sucrose in PBS overnight at 4°C, embedded in OCT and frozen at −20°C. For brain tissue, sections (40 um) were prepared with a cryostat. Sections were then washed and mounted on slides with DAPI fluoromount-G (Southern Biotech) or stained. For staining, free-floating sections were blocked (5% NGS in 0.1% PBST (0.1% Triton X-100 in PBS)) for 30 min at RT and incubated with primary antibodies overnight at 4°C. The next day, sections were washed 3x10 min with 0.1% PBST, incubated with secondary antibodies for 2 hours at RT, washed again 3 × 10 minutes with 0.1% PBST, and then mounted as above.

For peripheral sensory ganglia, ventral aspect of skulls and vertebral columns were dissected, post-fixed in 10% formalin overnight at 4°C, and washed 3 × 20 minutes with PBS at RT. Nodose ganglion and dorsal root ganglion were then dissected out and cryoprotected as described above. Ganglion sections (20 μm) were prepared with a cryostat, collected on slides, and dried overnight at RT before staining. Slides were washed 3 × 10min with 0.1% PBST and then stained as described above.

The following antibodies were used: chicken anti-GFP (Abcam, ab13970), 1:1000 in blocking solution; rabbit anti-Iba1 (Wako, 019-19741), 1:1000 in blocking solution; goat anti-chicken Alexa 488 (Invitrogen, A-11039), 1:500 in blocking solution; goat anti-rabbit Alexa 568 secondary antibody (Invitrogen, A-11036), 1:1000 in blocking solution.

For histologic characterization of Cre-dependent ribo-GCaMP in PVH, AAV5 encoding DIO-riboGCaMP6f or DIO-GCaMP6f (200 nL) was bilaterally injected into the PVH (−0.75 mm AP, ± 0.30 mm ML, −4.85 mm DV) of SIM1-Cre mice. For histologic characterization of ribo-GCaMP in medial prefrontal cortex (mPFC), hippocampus (HPC) and superior colliculus (SC), AAV encoding ribo-GCaMP6m or GCaMP6m (200-300 nL) was unilaterally injected into the mPFC (+1.5 mm AP, −0.35 mm ML, −2.6 mm DV), HPC(−1.8 mm AP, −1.0 mm ML, −2.2 mm DV), SC (0 mm AP (lambda), -∼0.6mm ML, −1.5 mm DV) and PVH (−0.75 mm AP, -0.25 mm ML, −4.8 mm DV). Mice were transcardially perfused 4 weeks after surgery.

For histologic characterization of the subcellular distribution of ribo-GCaMP in striatal Ntrk1 neurons, AAV9 encoding hSyn-DIO-riboGCaMP6m or hSyn-DIO-GCaMP6m (100 nL) was co-injected with AAV5 encoding EF1a-DIO-ChR2(H134R)-mCherry (100 nL) into the striatum (0.6 mm AP, ± 2.5 mm ML, 2.9 mm DV) of Ntrk1-Cre mice. Mice were transcardially perfused 2-4 weeks after viral injection. To reconstruct single Ntrk1-Cre neurons, a tiled Z stack image was taken for both the red (ChR2(H134R)-mCherry) and green (GCaMP6m or ribo-GCaMP6m) channels. The red channel was used to create a 3D mask based on pixel threshold and connectivity using FIJI (Schindelin et al., 2012). Then both the green and red fluorescence inside but not outside the mask were retained to show the relationship between the green channel and the shape of single cells. To trace the intensity of GCaMP6m or ribo-GCaMP6m along individual axons, we manually traced the axon of selected neurons in the red channel starting from the beginning of the axon. We then extracted the pixel intensity along the traced line to generate plot of green intensity versus distance from soma.

For histologic characterization of ribo-GCaMP after long-term expression in mPFC, AAV8 encoding ribo-GCaMP6m and GCaMP6m (200 nL each) were each injected into opposing hemispheres of mPFC (+1.5 mm AP, ± 0.35 mm ML, −2.6 mm DV). Mice were transcardially perfused 4, 6, 8 or 12 weeks after surgery.

Slice field stimulation

AAV encoding ribo-GCaMP6m or GCaMP6m (200 nL) was bilaterally injected into the HPC (−1.8 mm AP, ± 1.0 mm ML, −2.2 mm DV). Brains were sliced and recovered in NMDG solution (Ting et al., 2014). Recordings were made with standard ACSF (2 mM calcium) containing a cocktail of inhibitors to repress neurotransmission and thus network activity: 10 μM CNQX (Tocris, 0190), 10 μM (R)-CPP (Tocris, 0247), 10 μM Gabazine (Tocris, 1262) and 1000 μM (S)-MCPG (Tocris, 0337) (Wardill et al., 2013). Fluorescence signals were recorded using a digital CCD camera (Hamamatsu, ORCA-ER) mounted on an Olympus upright microscope (BX51WI). Micro-manager software (version 1.4) was used as microscope control interface (Edelstein et al., 2014). Slices were imaged (5 ms exposure time; 20 Hz) with 470 nm excitation through a filter set (U-N41 017, E.X. 470 nm, B.S. 495 nm, E.M. 5, Olympus). Field stimulation (30-40V) was delivered through parallel platinum wires (Warner Instruments, RC-49MFS) from a stimulation isolator (A.M.P.I, ISO-Flex). The stimulation pattern (80 Hz, 5 ms pulse width) was generated by Digidata 1550 (Molecular Devices) and pClamp 10.5 software (Molecular Devices). The same stimulation and recording parameters were used to evaluate the response of ribo-GCaMP6m and GCaMP6m. Rise time constant and decay time constant were defined, respectively, as the time that it takes fluorescence to reach 50% of peak fluorescence from the onset of stimulation, and the time to decay to 50% of peak fluorescence from the peak of fluorescence.

Slice two-photon recording

All cells recorded were Type 2 L5 pyramidal neurons as determined by I_h mediated sag and rebound (Gee et al., 2012). Recordings were made with standard ACSF (2 mM calcium) and k-gluconate internal with EGTA omitted. Internal contained 20 μM for cell visualization. Cells were held a −68 mV and stimulated with variable number of spikes at 100 Hz while simultaneously imaging with 2-Photon linescans using 920 nm stimulation. Imaging was first conducted at the soma, then the apical dendrite at distances of 20, 50, 100, 150, and 200 μm, and then the basal dendrites at 20, 50, and 100 μm. Z stacks of the entire cell were then taken to recover the full dendritic morphology. Baseline noise was calculated from the standard deviation of the fluorescent signal 100 ms before stimulus onset. Signal to noise was calculated as the peak dF/F divided by the baseline noise.

Cranial window surgery and headfixed two-photon imaging

Experiments were conducted on adult C57BL6/J mice (males, age > 8 weeks). During surgery a custom titanium head plate (eMachineshop) was attached to the skull using dental cement (Metabond, Parkell), and a 3 mm diameter craniotomy was made over visual cortex (0.8 mm anterior from lambda and 2.5 mm lateral from bregma). In the middle of the craniotomy, virus (AAV9-riboGCaMP6m or AAV9-GCaMP6m) was injected at two sites (−0.6 mm ventral from skull surface, 0.8 and 1.0 mm anterior from lambda, volume: 150 nL at each site, rate: 15 nL/min). A window plug made from two 3 mm diameter coverglasses glued to a 5 mm diameter coverglass was placed over the craniotomy and fixed in place using dental cement. Imaging experiments began 3 weeks after window implantation.

Mice were headfixed in a body tube under a Nikon 16X objective and imaged using a resonant scanning two-photon microscope (Neurolabware). Images were acquired at a rate of 15.49 Hz with a field of view of 1.2 mm by 0.9 mm mm. We found that ribo-GCaMP6m was dimmer than GCaMP6m *in vivo* under the same laser setting. To match the fluorescence intensity and thus enable fair cross-correlation comparison, laser power was set to be higher when imaging ribo-GCaMP6m than GCaMP6m preps (67 mW

Please cite this article in press as: Chen et al., Soma-Targeted Imaging of Neural Circuits by Ribosome Tethering, Neuron (2020), https://doi.org/10.1016/j.neuron.2020.05.005

versus 28 mW). Pixel size was calibrated to be ~1.9 μm x 1.9 μm. Imaging in layer 2/3 was performed 200 μm below the pial surface. Moving bar stimuli were generated using Psychtoolbox3 (MATLAB) and presented on an LCD screen positioned 20 cm away from the mouse (Kleiner et al., 2007). Bars were 5-7° wide and drifted at 18-22° s-1. Bars were white against a gray background. In a separate series of experiments, full-screen moving grating stimuli were presented with a cycle length of 10-15° and a temporal frequency of 2 Hz. All stimuli were presented in a pseudorandom sequence (sampling without replacement) with interspersed breaks (8.4 s).

For data analysis, lateral brain motion was corrected using NoRMCorre (MATLAB) (Pnevmatikakis and Giovannucci, 2017). Neuron identification, segmentation and fluorescent signal extraction were performed using Suite2P (Python) (Pachitariu et al., 2017). Identified ROIs were further manually screened. Suite2P computed the neuropil signal for each ROI, which is defined as the weighted average signal of all pixels surrounding each ROI; the minimal width of the donut-shaped surrounding neuropil area is defined as 100 pixels (~190 μm).

To subtract the neuropil signals from the soma signal, we used the equation suggested by Suite2P, that is $F_{subtracted} = F_{soma} - 0.6\ x\ F_{neuropil}$. Data shown in the following figures underwent neuropil subtraction for both ribo-GCaMP6m and GCaMP6m: Figures 5C–5E and S3B. Some data shown in those figures also underwent neuropil subtraction, and the details are indicated in the following figure legends: Figures 5B, 5F–5I, S3C, and S6D. Note that the neuropil subtraction has little effect on the ribo-GCaMP6m results and is applied primarily so that ribo-GCaMP6m can be compared to GCaMP6m using a standard two-photon data analysis procedure.

To normalize the fluorescent signal of each ROI, the signal of each frame was z-scored as $Fz = (F_{eachframe}\text{-}mean(F_{local}))/std(F_{local})$. F_{local} is the fluorescence signal of a 1-minute time window centering each frame. When calculating z-score for the first or last N frames (N < 60), a moving window with size *60-N* was used.

To compute the response of a neuron to each visual stimulus, a time window of two seconds before the onset of each stimulus was defined as the pre-stim period, and a 5 s (for drifting grating stimuli) or 7 s (for drifting bar stimuli) time window after each stimulus was defined as the post-stim period. The response of the neuron to the stimulus was calculated as the signal maximum minus the median signal during the pre-stim period. To identify orientation-tuned neurons, we used 1-way ANOVA to test whether a neuron responds differentially to visual stimuli with different orientations. Neurons with P value < 0.01 were defined as orientation-selective (Dana et al., 2019). The stimuli that triggered the maximal neural response are defined as having the preferred angle.

To perform segmentation based on static images, we first averaged z-projection of each video of drifting bar experiment and enhanced the local contrast by applying *adapthisteq* function (MATLAB). We then used NeuroSeg (MATLAB), a segmentation algorithm that solely based on static image, to generate ROIs (Min sigma = 1; Max sigmal = 3; Min area = 12) (Guan et al., 2018). All automatically generated ROIs are used in the comparison without manual selection.

Microendoscope imaging and ingestive behavior

For microendoscope experiments, mice were prepared based on published protocols (Flusberg et al., 2008; Ghosh et al., 2011; Resendez et al., 2016). In brief, AAV encoding ribo-GCaMP6m (200 nL) was unilaterally injected into the mPFC (−1.5 mm AP, −0.35 mm ML, −2.6 mm DV). A Ø500 μm gradient index (GRIN) lens (6.1 mm length; Inscopix) was then placed 0.10 mm above the injection site in the same surgery. Baseplates (Inscopix) were then mounted 4-8 weeks after initial surgery. Mice were allowed to recover for 2 weeks after baseplating and were habituated to handling and behavioral apparatus for another week. During the experiment, mPFC neurons of each mouse were recorded through a miniature microscope (Inscopix) using nVista software (https://www.inscopix.com/nvista) with identical settings (20 Hz, 20% LED power, 3.0 gain). After a 10-minute baseline measurement, the mice were allowed to consume liquid food (Ensure). The mice were either fed or food deprived for 24 hours before the start of each experiment.

To analyze microendoscope data, videos were first pre-processed (spatial downsample by a factor of 2; temporally downsample by a factor of 5) and motion-corrected using Mosaic software MATLAB API suite (https://support.inscopix.com/mosaic-workflow). Activity traces for individual neurons were then extracted from these videos using the constrained nonnegative matrix factorization - endoscope (CNMF_E) pipeline (MATLAB) (Zhou et al., 2018). Consummatory events were recorded by a capacitance-based (https://www.arduinolibraries.info/libraries/capacitive-sensor) contact lickometer custom build with microcontrollers (Arduino Uno) connected to the data acquisition box of mini-endoscope.

Calcium imaging in *Caenorhabditis elegans*

For ASH and AFD imaging, well-fed young adult worms were immobilized in custom-built microfluidic devices (Chronis et al., 2007) in S buffer (100 mM NaCl, 50 mM KH_2PO_4, pH 6.0) with addition of 0.02% (m/v) tetramisole hydrochloride (Sigma-Aldrich, St. Louis, MO). Ribo-GCaMP6m (GCaMP6m C-terminal fusion with RPL-1) or soluble GCaMP6m was expressed in the *C. elegans* ASH sensory neuron under control of the *sra-6* promoter. Worms were stimulated with 0.5 M sodium chloride delivered to the nose of the animal for 10 s (one pulse). ASH imaging was preceded by a 30 s exposure to blue light to reduce intrinsic light response (Hilliard et al., 2005; Ward et al., 2008). Each worm was subjected to two stimulatory pulses of 0.5 M sodium chloride with a 1 min interval between the pulses. For AFD imaging, GCaMP6m-RPL-1 fusion was expressed in the AFD sensory neuron under control of the *ntc-1* promoter. Heat stimulation was performed by delivering pre-warmed buffer (~30°C) to the nose of the animal for 10 s (one pulse). An in-line solution heater (Warner Instruments, SF-28) was incorporated into the setup to provide pre-warmed buffer flow and buffer temperature at the device was measured using a handheld thermocouple thermometer. Each worm was subjected to three stimulatory warm buffer pulses with a 1 min interval between the pulses. GCaMP fluorescence was visualized by illumination with a LED lamp (X Cite©

120LED, Excelitas Technologies, 480/30 nm excitation filter, 535/40 nm emission filter, Chroma). Images were collected on Axio Observer A1 microscope (Zeiss) at 10 frames per second using a 63x, 1.4 NA objective and a CMOS camera (ORCA-Flash4.0, Hamamatsu). Fluorescent signal modulation over the period of acquisition was analyzed using Fiji software by defining the soma or dendrite and subtracting the background fluorescence (Reilly et al., 2017). Fluorescence intensity was normalized to the baseline signal (F0) during the last 1 s in control buffer prior to stimulus delivery and further analyzed using a custom written Python script. Data are plotted as mean ± SEM (shaded region).

For whole-brain imaging of head ganglia neurons, ribo-GCaMP6m or nls-GCaMP6m were expressed using the pan-neuronal *tag-168* and *rab-3* promoters, respectively, in the *lite-1* genetic background with pan-neuronally expressed nuclear RFP markers.

Calcium imaging recordings were made using a Nikon Ti Microscope with Andor Zyla 5.5 sCMOS camera. The worm was immobilized in a microfluidic chip with addition of 1% tetramisole as described (Kato et al., 2015). Recordings were started within 5 min after removal from food. The head of the worm was imaged for 5-18 minutes using a 40x objective and collecting 10-24 z stacks of 2 μm step size to cover the thickness of the worm, with 33.3 or 50 frames per second. The center of the individual regions of interest (ROIs) were manually selected from each soma (ribo-GCaMP6m) or nucleus (nls-GCaMP6m) using Fiji software, and subsequent analysis was performed by a custom-written Python script. The fluorescence intensity from a square of 3x3 pixel areas surrounding the center of the ROI was measured and delta F/F_0 was calculated by defining baseline signal (F_0) as the mean intensity over the whole trace.

Rise time measurement and comparison

Rising transients in extracted neural timeseries were computationally detected using a peak finding algorithm followed by detection of onset and termination frames of rise periods using first and second derivative threshold criteria on smoothed timeseries, as implemented in the Python notebook included in Key Resources Table. To estimate the temporal differences between the ribo-GCaMP6m and nls-GCaMP6m indicators, epochs from ribo-GCaMP6m recordings containing rise transients were extracted and convolved with a first-order linear filter with a time constant of tau. Rise times were then measured in the resulting simulated trace excerpts. An optimal tau was determined by minimizing the error between a histogram of the simulated trace excerpts and a histogram of the nls-GCaMP6m rise times. This optimal tau gives an estimate of the temporal blurring effects of the nls-GCaMP6m versus the ribo-GCaMP6m indicator.

QUANTIFICATION AND STATISTICAL ANALYSIS

Statistical analyses and linear regressions were performed using Prism 7 (https://www.graphpad.com/scientific-software/prism). Values are reported as mean ± s.e.m. (error bars or shaded area), represented as black brackets in bar graphs and shaded areas in PSTH plots. In figures with linear regressions, the dotted lines represent the 95% confidence interval for the line-of-best-fit. P values for pairwise comparisons were performed using a two-tailed Student's t test. P values for comparisons across multiple groups were performed using ANOVA and corrected for multiple comparisons using the Holm-Šídák method. *$p < 0.05$, **$p < 0.01$, ***$p < 0.001$, ****$p < 0.0001$. N values and definitions can be found in the figure legends. No statistical method was used to predetermine sample size. Randomization and blinding were not used. Here is a full list of published open-source packages/software used in this study:

FIJI (Figures 1, 2, 4, 7, S1, S3, and S4): https://imagej.net/Fiji/Downloads (Schindelin et al., 2012)
Psychtoolbox3 (Figures 5 and S3): https://github.com/Psychtoolbox-3/Psychtoolbox-3 (Kleiner et al., 2007)
NormCorre (Figures 5 and S3): https://github.com/flatironinstitute/NoRMCorre (Pnevmatikakis and Giovannucci, 2017)
Suite2P (Figures 5 and S3): https://github.com/cortex-lab/Suite2P (Pachitariu et al., 2017)
Capacitive Sensing Library (Figure 6): https://playground.arduino.cc/Main/CapacitiveSensor/
CNMF_E (Figure 6): https://github.com/zhoupc/CNMF_E (Zhou et al., 2018)
PCA/ICA (Figure 6): https://github.com/mukamel-lab/CellSort (Mukamel et al., 2009)
NeuroSeg (Figure S3): https://github.com/baidatong/NeuroSeg (Guan et al., 2018)